BJR

Received: 26 January 2014 | Revised: 22 June 2014 | Accepted: 9 July 2014

doi: 10.1259/bjr.20140091

Cite this article as:
Ganesan K, Bydder GM. A prospective comparison study of fast T_1 weighted fluid attenuation inversion recovery and T_1 weighted turbo spin echo sequence at 3 T in degenerative disease of the cervical spine. Br J Radiol 2014;87:20140091.

FULL PAPER

A prospective comparison study of fast T_1 weighted fluid attenuation inversion recovery and T_1 weighted turbo spin echo sequence at 3 T in degenerative disease of the cervical spine

[1]K GANESAN, MB BS, DNB and [2]G M BYDDER, MB ChB

[1]Department of MRI, Jaslok Hospital and Research Center, Mumbai, Maharashtra, India
[2]MR3T Research Laboratory, Department of Radiology, University of California, San Diego, CA, USA

Address correspondence to: Dr Karthik Ganesan
E-mail: drkarthikg@gmail.com

Objective: This study compared T_1 fluid attenuation inversion recovery (FLAIR) and T_1 turbo spin echo (TSE) sequences for evaluation of cervical spine degenerative disease at 3 T.

Methods: 72 patients (44 males and 28 females; mean age of 39 years; age range, 27–75 years) with suspected cervical spine degenerative disease were prospectively evaluated. Sagittal images of the spine were obtained using T_1 FLAIR and T_1 TSE sequences. Two experienced neuroradiologists compared the sequences qualitatively and quantitatively.

Results: On qualitative evaluation, cerebrospinal fluid (CSF) nulling and contrast at cord–CSF, disc–CSF and disc–cord interfaces were significantly higher on fast T_1 FLAIR images than on T_1 TSE images ($p < 0.001$). No significant difference was seen between the sequences in evaluation of neural foramina and bone–disc interface. On quantitative evaluation, the signal-to-noise ratios of cord and CSF on fast T_1 FLAIR images were significantly higher than those on T_1 TSE images ($p < 0.05$). Contrast-to-noise ratios (CNRs) of cord to CSF on T_1 FLAIR images were significantly higher than those of T_1 TSE images ($p < 0.05$). CNRs of bone to disc for T_1 weighted TSE images were significantly higher than those of T_1 FLAIR images ($p < 0.05$).

Conclusion: At 3 T, T_1 FLAIR imaging is superior to T_1 TSE for evaluating cervical spine degenerative disease, owing to higher cord–CSF, disc–cord and disc–CSF contrast. However, intrinsic cord contrast is low on T_1 FLAIR images.

Advances in knowledge: T_1 FLAIR is more promising and sensitive than T_1 TSE for evaluation of degenerative spondyloarthropathy and may provide a foundation for development of MR protocols for early detection of degenerative and neoplastic diseases.

T_1 weighted turbo spin echo (TSE) sequence is a routine sequence included in our protocol to image the cervical spine at 3 T. Prolongation of tissue spin lattice relaxation times at 3 T relative to those at 1.5 T results in reduced contrast between the spinal cord and cerebrospinal fluid (CSF) on T_1 weighted TSE (T_1 TSE) images.[1–3] To overcome this problem, T_1 weighted fluid attenuated inversion recovery (T_1 FLAIR) sequences are frequently used for imaging the spine.[1,4] Inversion recovery sequences provide increased tissue contrast vis-à-vis spin echo sequences. These were initially developed for examination of the spine at 1.5 T[4] and were designed to null the signal from CSF and maximize contrast between different pairs of tissues, which are commonly seen on spine images as well as between tissue and CSF. Typical combinations of T_1 FLAIR sequence of repetition time (TR), inversion time (TI) and echo time (TE) at 1.5 T are 2000, 862 and 10 ms[4] and 2000, 862 and 6 ms[5] and at a lower field strength (0.2 T) 970, 450 and 29 ms, respectively.[6] For operation at 3 T, longer values of TR, TI and TE are generally employed, *e.g.* 2675, 2000 and 17 ms.[1] Longer TRs are acceptable for the T_1 FLAIR sequence at 3 T, and, by mathematical simulation, Oda et al[7] showed a wide but optimum range of TRs between 2400 and 3900 ms at 3 T. Although T_1 FLAIR sequences are commonly used in the spine and are said to provide excellent delineation of CSF, bone and disc bone interfaces at 3 T,[1–3] to date there has been little critical evaluation of their performance. Most of the articles have dealt with the role of T_1 FLAIR sequence in imaging degenerative disease of the lumbar spine,[5,8] wherein suppression of the abundant quantity of CSF within the lumbar thecal sac would allow for greater tissue contrast and improved image quality. On the contrary, the relative paucity of the sleeves of CSF surrounding the cervical cord would seem to present

a relative hindrance in the assessment of the cervical spine using the T_1 FLAIR sequence. In this article, we describe a prospective comparison of T_1 FLAIR and T_1 TSE sequences for evaluation of cervical spine degenerative disease at this field strength.

METHODS AND MATERIALS

72 consecutive patients (44 males and 28 females) with suspected cervical spine degenerative disease were prospectively evaluated. Cervical degenerative disease was suspected on the basis of clinical findings and plain radiographs of the cervical spine. Each patient underwent plain radiography in the anteroposterior and lateral projections. There was no history of trauma. The patients' age ranged between 27 and 75 years with a mean age of 39 years. All patients underwent MRI on a 3-T MAGNETOM® Trio MR system (Siemens Medical Solutions, Erlangen, Germany) using a spine array coil. The MRI protocol included the following sequences: T_1 FLAIR (TR/TI/TE = 3520/1450/7.7 ms; matrix = 384 × 270 pixels; acquisition time = 4 min 32 s; turbo factor = 7; bandwidth (BW) = 289 Hz per pixel) and T_1 TSE (TR/TE = 700/9.9 ms; matrix = 448 × 224 pixels; acquisition time = 2 min 48 s; turbo factor = 5; BW = 289 Hz per pixel). All sequences were obtained in the sagittal plane at the same imaging session. The remaining parameters for the T_1 TSE and T_1 FLAIR sequences were identical and included the following: slice thickness = 3 mm; interslice gap = 0 mm; number of slices = 11; and field of view = 28 × 22 cm.

Quantitative analysis

Quantitative analysis was performed on the scans of all 72 patients. The signal intensity (SI) of the cervical cord, vertebral bone marrow, discs, CSF and the standard deviation (SD) of the background noise were measured after drawing appropriately placed regions of interest. These were similar in size and placed in identical locations on both the T_1 FLAIR and T_1 TSE images in each patient. From the SI values of the observed structures, the following ratios were calculated: signal-to-noise ratio (SNR) of the spinal cord and CSF, contrast-to-noise ratio (CNR) between CSF and spinal cord, as well as between bone marrow and the adjacent disc. SNRs were calculated as $SNR = SI_{tissue\ or\ fluid}/SD$ of background noise. CNRs were calculated as $(SI_{tissue\ or\ fluid1} - SI_{tissue\ or\ fluid2})/SD$ of background noise.

Qualitative analysis

In all 72 patients, the T_1 FLAIR and T_1 TSE sequences were compared qualitatively. The images from both sequences were optimized for window width and level. Two experienced neuroradiologists (20 years' and 5 years' experience, respectively) evaluated the results from both sequences independently in all 72 patients on two occasions 1 week apart. The neuroradiologists graded the two sequences on a scale of 0–3 (0, not visualized; 1, poor; 2, average; and 3, good) for the following features: image quality, CSF nulling, cervical cord–CSF contrast, cervical disc–CSF contrast, disc–cervical cord contrast, neural foramina visibility and bone marrow–disc contrast. More generalized abnormalities of the cervical spine such as abnormal curvature, vertebral body wedging or fusion, discovertebral junction irregularities and the presence of other disease were also evaluated.

Statistical analysis

Statistical analysis was performed using SPSS® for Windows v. 15.0 (SPSS Inc., Chicago, IL). The statistical significance of the qualitative and quantitative data was determined using the Wilcoxon's signed-rank test. p-values <0.05 were considered to be statistically significant.

RESULTS

7 of the 72 patients had normal cervical spine MR images. 64 patients had evidence of mild to severe cervical spine degenerative disease (Figures 1–5). The spectrum of imaging findings included the following: disc bulge ($n = 17$), disc

Figure 1. (a, b) 42-year-old male with mild cervical disc bulges indenting the anterior subarachnoid space. Note the greater cerebrospinal fluid (CSF) suppression (white arrow) and improved contrast of the CSF boundaries (black arrow) on the T_1 fluid attenuation inversion recovery image (b) as compared with the T_1 turbo spin echo image (a).

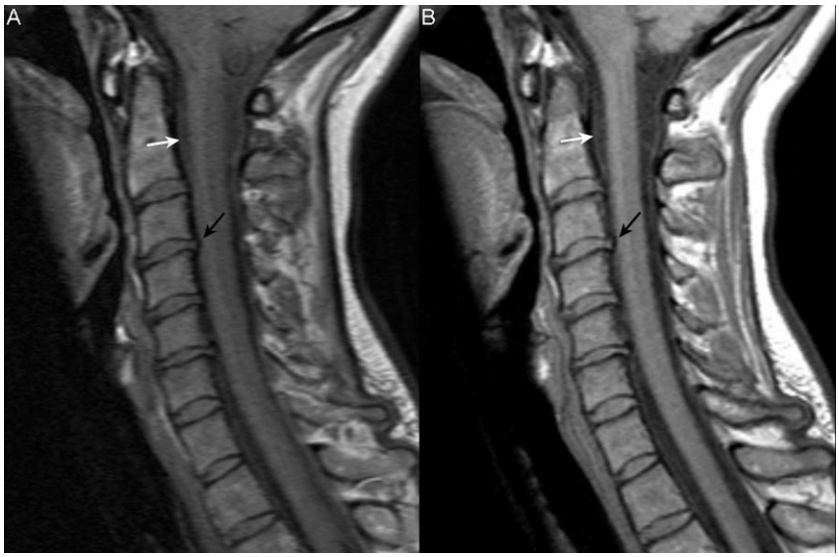

Figure 2. (a, b) 68-year-old female presented with acute radiculopathy. A large C4/5 disc central extrusion compresses the cervical cord and exiting right C5 nerve root (not shown). Note the greater contrast of the cerebrospinal fluid (CSF) boundary results in a more distinct disc-CSF interface (white arrows) on the T_1 fluid attenuation inversion recovery image (b) as compared with the T_1 turbo spin echo image (a).

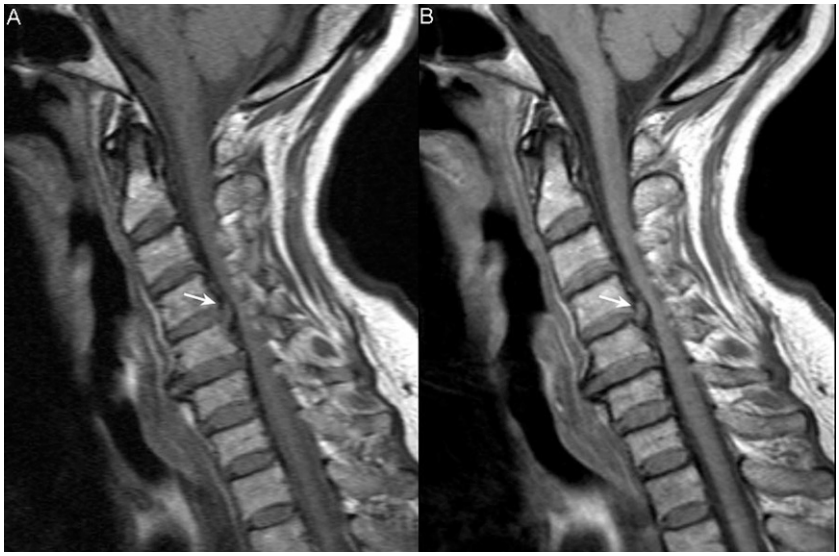

herniation ($n = 47$), discovertebral junction abnormalities ($n = 44$), osteophytes ($n = 39$), neural foraminal narrowing ($n = 26$), cord compression without signal alteration in the cord ($n = 7$), cord compression with focal areas of myelomalacia ($n = 3$) and curvature abnormalities ($n = 5$) (Figures 1–5). Mild forms ($n = 12$) revealed only indentation of the anterior subarachnoid space without obliteration of the CSF sleeve. Moderate forms ($n = 34$) revealed obliteration of the subarachnoid space without cord compression, with mild foraminal compromise. Severe forms ($n = 19$) revealed cord compression or displacement with exiting nerve root impingement and foraminal stenosis. One patient had a posterior epidural cervical haematoma from rupture of a cervical arteriovenous malformation, which was associated with cervical cord compression (Figure 6).

Quantitative analysis

The results of the quantitative analysis are shown in the form of mean ± SD in Table 1. SNRs of both the spinal cord and CSF obtained with the T_1 FLAIR sequence were significantly higher than those obtained with the T_1 TSE sequence ($p < 0.05$). The CNR between cervical cord and CSF was significantly higher with the T_1 FLAIR sequence than with the T_1 TSE sequence ($p < 0.05$). However, the CNR for bone marrow to cervical disc was significantly higher with the T_1 TSE sequence than with the T_1 FLAIR sequence (<0.05).

Figure 3. (a, b) 75-year-old female presented with chronic neck pain due to long-standing degenerative cervical spondylosis. No significant difference was noted in the evaluation of discovertebral anomalies on both sequences (white arrows).

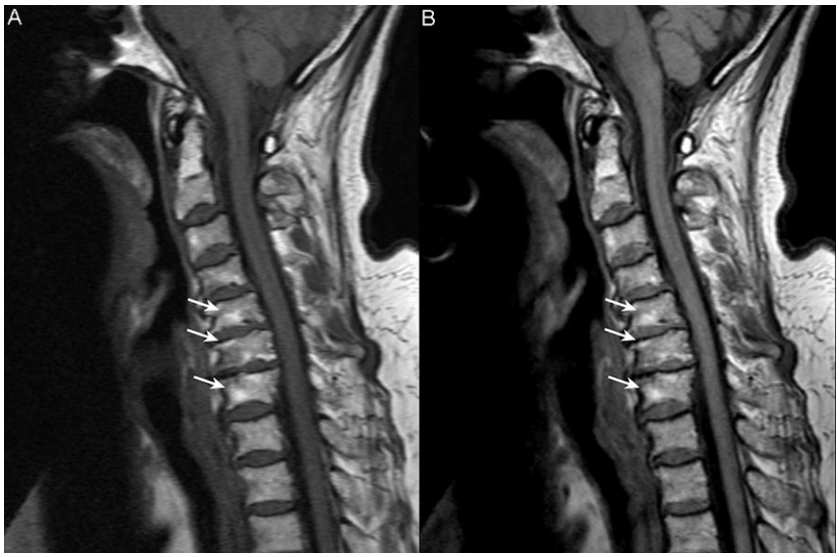

Figure 4. (a, b) 53-year-old female with cervical degenerative spondylosis. No significant difference was noted in the evaluation of neural foramina on both sequences (white arrows).

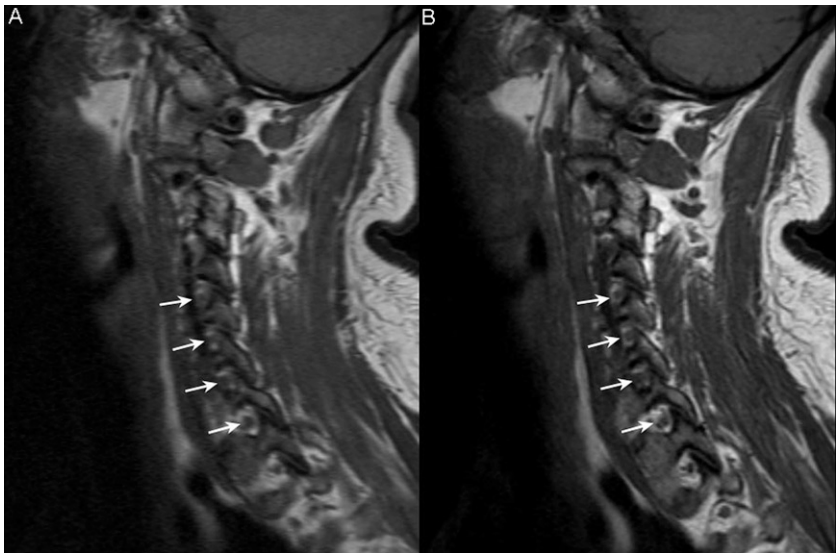

Qualitative analysis

The results of the qualitative analysis of data obtained from 72 patients are summarized in Table 2. The T_1 FLAIR sequence was superior to the T_1 TSE sequence in nulling the CSF. The contrast at the cervical cord–CSF, cervical disc–CSF and disc–cord interfaces were significantly higher with the T_1 FLAIR sequence. The T_1 FLAIR sequence was not significantly better than T_1 TSE sequence for evaluation of discovertebral abnormalities and neural foramina. Intrinsic cervical cord contrast was greater with the T_1 TSE sequence than with the T_1 FLAIR sequence in a case of compressive myelopathy secondary to a posterior epidural haematoma, where cervical

Figure 5. (a–c) 54-year-old male presented with tingling and numbness in bilateral lower limbs. T_2 turbo spin echo (TSE) sagittal image (a) shows a discrete focus of myelomalacia at the C3/4 level in the posterior aspect of the cord (white arrow). Note the poor visualization of the myelomalacia (arrows) on the T_1 TSE (b) image as compared with the T_1 fluid attenuation inversion recovery (c) image.

Figure 6. (a–c) 32-year-old male with a posterior epidural haematoma due to a ruptured dural arteriovenous malformation causing compressive myelopathy. T_2 turbo spin echo (TSE) sagittal image (a) shows a posterior epidural haematoma (arrow) causing diffuse cord oedema (white arrow). Note the relatively poor visualization of the cord oedema on the T_1 fluid attenuation inversion recovery (c) image as compared with T_1 TSE (b) image.

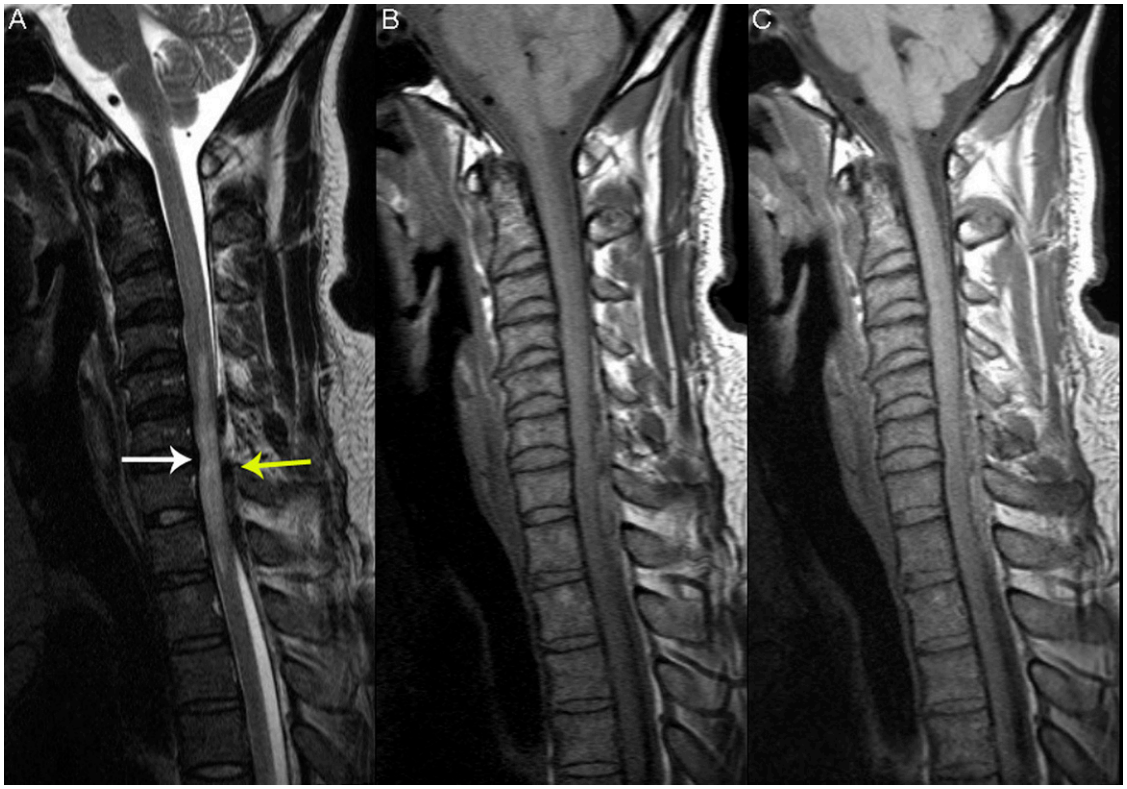

cord oedema was better visualized with the T_1 TSE sequence than with the T_1 FLAIR sequence. However, in a case of long-standing compressive myelopathy, focal areas of myelomalacia were better visualized with the T_1 FLAIR sequence than with the T_1 TSE sequence.

DISCUSSION

The role of FLAIR sequence in imaging the brain at 3 T has been well described in the literature. However, its role in routine clinical imaging of the spine has not received much attention. TSE techniques can be applied to T_1 FLAIR sequences to make acquisition times comparable to T_1 weighted TSE sequences. Fast T_1 FLAIR sequences have been preferred to T_1 weighted spin echo imaging in the brain owing to their superior grey–white contrast, excellent nulling of CSF and improved contrast between the lesion and normal structures.[6,9] At 3 T, prolongation of T_1 relaxation times results in reduced T_1 contrast resulting in increased SI of the CSF. At 3 T, the improved nulling of CSF provided by T_1 FLAIR imaging provides excellent tissue contrast and better delineation of the tissue interfaces.

Both the quantitative and qualitative findings support the view that contrast involving CSF boundaries is generally increased with T_1 FLAIR sequences, and this is of considerable importance in defining the boundaries of the cord and recognizing extra-axial disease. The SNRs of CSF and cervical cord, and the CNR of cervical cord to CSF were significantly greater on the T_1 FLAIR sequence. The qualitative significance of these results meant improved conspicuity at the following anatomical locations: cervical cord–CSF, cervical disc–CSF and cervical disc–cervical cord interfaces. This allowed the neuroradiologists to identify normal interfaces, detect disc protrusions and differentiate between cord indentation and compression.

The higher SI of the cord combined with greater CSF signal reduction with the T_1 weighted FLAIR sequence provided better conspicuity for myelomalacia. However, in one case of posterior epidural haematoma secondary to spontaneous rupture of a dural arteriovenous (AV) fistula, cord oedema was poorly visualized on the T_1 FLAIR sequence compared with the T_1 TSE sequence. This finding raises the possibility that T_1 FLAIR sequence may be less effective in evaluating intramedullary lesions such as cord oedema, multiple sclerosis plaques and tumours.

In our study, the SNR of CSF was higher on T_1 FLAIR compared with the T_1 TSE images. The use of slice-selective radiofrequency (RF) pulse variant of T_1 FLAIR sequence is the likely explanation for this finding. T_1 FLAIR sequences may be performed using either non-slice-selective or slice-selective RF pulses. Slice-selective T_1 FLAIR sequence is prone to CSF flow effects caused by pulsatile CSF flow displacing inverted spins and replacing them with non-inverted spins from outside the

Table 1. Results of the quantitative analysis obtained from 72 patients

Sequence	SNR of cord	SNR of CSF	CNR of cord–CSF	CNR of bone–disc
T_1 weighted turbo spin echo	50.21 ± 7.32	37.29 ± 4.36	12.92 ± 3.37	15.30 ± 7.82
T_1 weighted fluid attenuation inversion recovery	95.37 ± 11.36	50.05 ± 9.37	45.32 ± 10.24	7.19 ± 10.6

CSF, cerebrospinal fluid; CNR, contrast-to-noise ratio; SNR, signal-to-noise ratio.

slice. This oscillatory motion may be responsible for the higher SNRs of CSF on T_1 weighted FLAIR images.[4] Use of non-slice-selective RF pulses in T_1 weighted FLAIR sequences would reduce CSF pulsation effects; however, each slice is then scanned with slightly different TI values, resulting in variation in image contrast.

The inversion times usually used with T_1 FLAIR sequences at 0.2–1.5 T are generally a little less than half the TR[4,6] as were the values used in this study at 3 T (TR = 3520 ms; TI = 1450 ms); however, the published values for TR (2675 ms) and TI (2000 ms) in a previous study of the cervical spine at 3 T differ from this rule.[1] There is a relative time penalty (4 min 32 s for T_1 FLAIR, 2 min 48 s for T_1 TSE) in order to achieve the generally superior contrast of the T_1 FLAIR sequence.

In clinical practice, the cervical spine is usually evaluated with the following sequences: two dimensional (2D) sagittal T_1 and T_2 weighted TSE sequences, 2D axial T_2 weighted TSE sequence and 2D or three dimensional axial T_2 weighted gradient echo sequence to differentiate disc material and osteophytes. One of the principal roles of MRI is to diagnose disc herniation, which may or may not be contiguous with the parent disc and free fragments are occasionally noted. The herniated material appears isointense to the parent disc on T_1 and T_2 weighted sequences. However, T_1 weighted TSE sequences often display poor image contrast and provide very little additional clinical information in this situation.

The T_1 dependent contrast produced by the T_1 FLAIR sequence is generally greater than the equivalent T_1 weighted spin-echo or fast spin-echo sequence and has similarities to the balanced inversion recovery sequence.[10] This generally results in lower SI for longer T_1 tissue in the spinal cord. This contrast is opposed by the T_2 weighting that is generally minimal with the short TEs usually used with the sequence. The cystic component is likely to result in lower signal from myelomalacia, but the relative lack of contrast in cord oedema is an unusual finding with the T_1 FLAIR sequence. T_1 FLAIR sequences provide CSF nulled images, which have been reported to be useful to assess intraspinal cord cysts, tumours, syrinxes and multiple sclerosis plaques.[4] The superior tissue contrast allows for sharper delineation of interfaces between soft tissue/CSF–bone or disc/CSF as well as abnormal/normal tissue interface, as reported by Shapiro.[1] Lavdas et al[8] reported that the T_1 FLAIR images provided a superior CNR over T_1 weighted FSE images in 16 cases of metastatic lesions to the vertebral body, which allowed for accurate assessment of the expansion of the lesion within the spinal canal. The results of our data support the analysis that T_1 FLAIR sequence is superior to T_1 weighted TSE sequence in providing better CSF nulled images, thereby improving the contrast at the interface of the bone–CSF or the disc–CSF.

CONCLUSION

The results of our study show that T_1 FLAIR sequence has definite advantages compared with the T_1 TSE sequence at 3 T. T_1 FLAIR sequence at 3 T had higher SNRs for cord, greater CSF nulling, greater CNRs for cord–CSF with better visualization of disc–cord and cord–CSF interfaces with normal bone–disc CNRs. In the evaluation of discovertebral abnormalities and the neural foramina, both sequences were similar. Intramedullary CSF intensity lesions such as myelomalacia may be better depicted with the T_1 FLAIR sequence. However, the T_1 FLAIR sequence seems less likely to be useful in clinical situations associated with intramedullary lesions such as cord oedema.

Table 2. Results of the qualitative analysis obtained form 72 patients

Imaging criteria	T_1 FLAIR *vs* T_1 TSE	Significance
CSF nulling	T_1 FLAIR superior to T_1 TSE	$p < 0.05$
Cord–CSF interface	T_1 FLAIR superior to T_1 TSE	$p < 0.05$
Disc–CSF interface	T_1 FLAIR superior to T_1 TSE	$p < 0.05$
Disc–cord interface	T_1 FLAIR superior to T_1 TSE	$p < 0.05$
Neural foramina evaluation	T_1 FLAIR similar to T_1 TSE	–
Bone–disc interface	T_1 FLAIR similar to T_1 TSE	–

CSF, cerebrospinal fluid; FLAIR, fluid attenuation inversion recovery; TSE, turbo spin echo.

REFERENCES

1. Shapiro MD. MR imaging of the spine at 3T. *Magn Reson Imaging Clin N Am* 2006; **14**: 97–108. doi: 10.1016/j.mric.2006.01.005
2. Tanenbaum LN. Clinical 3T MR imaging: mastering the challenges. *Magn Reson Imagin Clin N Am* 2006; **14**: 1–15. doi: 10.1016/j.mric.2005.12.004
3. Fries P, Ruye VM, Kirchin MA, Watkins DM, Buecker A, Schneider G. Magnetic resonance imaging of the spine at 3 Tesla. *Semin Musculoskelet Radiol* 2008; **12**: 238–52. doi: 10.1055/s-0028-1083107
4. Melhem ER, Israel DA, Eustace S, Jara H. MR of the spine with a fast T1-weighted fluid attenuated inversion recovery. *Am J Neuroradiol* 1997; **18**: 447–54.
5. Erdem LO, Erdem CZ, Acikgoz B, Gundogdu S. Degenerative disease of the lumbar spine: a prospective comparison of T1-weighted fluid attenuation inversion recovery and T1-weighted turbo spin echo MR imaging. *Eur J Radiol* 2005; **55**: 277–82.
6. Hori M, Okubo T, Uozumi K, Ishigame K, Kumagai H, Araki T. T1-weighted fluid attenuated inversion recovery at low-field strength: a viable alternative for T1-weighted intracranial imaging. *AJNR Am J Neuroradiol* 2003; **24**: 648–51.
7. Oda S, Miki H, Kikuchi K, Hiratsuka Y, Murase K, Mochizuki T. Optimization of scan parameters for T1 FLAIR imaging at 1.5 and 3T using computer simulation. *Magn Reson Med Sci* 2013; **12**: 183–91.
8. Lavdas E, Vlychou M, Arikidis N, Kapsalaki E, Roka V, Fezoulidis IV. Comparison of T1-weighted fast spin echo and T1-weighted fluid attenuation inversion recovery images of the lumbar spine at 3.0 Tesla. *Acta Radiol* 2010; **51**: 290–5.
9. Rydberg JN, Hammond CA, Huston J 3rd, Jack CR Jr, Grimm RC, Riederer SJ. T1-weighted MR imaging of the brain using a fast inversion recovery pulse sequence. *J Magn Reson Imaging* 1996; **6**: 356–62.
10. Yokoo T, Bae WC, Hamilton G, Karimi A, Borgstede JP, Bowen BC, et al. A quantitative approach to sequence and image weighting. *J Comp Assist Tomogr* 2010; **34**: 317–31. doi: 10.1097/RCT.0b013e3181d3449a